Available online at www.sciencedirect.com
ScienceDirect
Vision Research 47 (2007) 1411–1423
Vision Research
www.elsevier.com/locate/visres

An oblique effect for transparent-motion detection caused by variation in global-motion direction-tuning bandwidths

John A. Greenwood *, Mark Edwards

School of Psychology, The Australian National University, Canberra 0200, Australia

Received 22 August 2006; received in revised form 15 December 2006

Abstract

Despite evidence for the broad direction tuning of global-motion detectors, transparent motion can be detected with comparatively small angular separations. The exact means by which this broad population response is decoded to yield multiple signal directions remains unclear. Consequently, we sought to determine the relationship between angular separation thresholds for transparent motion and the direction-tuning bandwidth of global-motion detectors. Angular separation thresholds were assessed around four axes of motion, with thresholds lower around cardinal axes than the oblique axes. This was also found with lowered signal intensities, despite larger differences between the component directions at threshold, indicating that the transparency oblique effect relies more on the mean direction than the components. Simulations with a model global-motion population suggest this is likely to arise from variation in direction-tuning bandwidths around the cardinal and oblique axes. In a second experiment, adaptation to oblique unidirectional motion produced threshold elevation for a wider range of test directions than adaptation to a cardinal direction. This is consistent with tighter direction tuning around cardinal axes and provides a basis for the transparent-motion oblique effect. Our narrow bandwidth estimates also suggest that transparent-motion detection could rely on bimodal activity within the global-motion stage.

Keywords: Motion perception; Transparency; Global motion; Bandwidth; Oblique effect

1. Introduction

Transparent motion, which occurs when multiple objects move through the same region of space without complete occlusion, presents two main problems for the motion-processing system. First, because distinct local-motion signals are spatially intermingled, signals with similar directions must be integrated at the same time as the segmentation of dissimilar signals (for review, see Snowden & Verstraten, 1999). The second problem occurs because motion-selective neurons each respond to a range of directions (e.g. Albright, 1984). Transparent-motion stimuli will thus produce broadly distributed population activity, from which two signal directions must be recovered. This is further complicated by recent work suggesting that population activity shifts from bimodal to unimodal at angular separations around 90° (Treue, Hol, & Rauber, 2000). Though unimodal activity should make transparency difficult to distinguish from unidirectional motion, angular separations as low as 25° can be detected (Braddick, Wishart, & Curran, 2002). To examine the mechanisms of transparent-motion detection under these circumstances, and evaluate the likely patterns of population activity produced by transparency, we sought to determine the relationship between angular separation thresholds and the direction tuning of global-motion detectors.

1.1. Transparent-motion detection

Because transparent motion is not seen when both signals are paired within local regions of the visual field, output from the initial local-motion stage appears to be insufficient for transparent-motion detection (Qian,

* Corresponding author. Fax: +612 6125 0499.
E-mail address: john.greenwood@anu.edu.au (J.A. Greenwood).

0042-6989/$ - see front matter © 2007 Elsevier Ltd. All rights reserved.
doi:10.1016/j.visres.2007.02.004

Andersen, & Adelson, 1994). Rather, local-motion signals from each of the component directions must be grouped appropriately within the global-motion stage. Accordingly, the limit of two transparent-motion signals that can be detected simultaneously is at least partly determined by global-motion detection thresholds (Edwards & Greenwood, 2005). This limit can be extended by distributing transparent-motion signals across multiple global-motion systems tuned to either speed (Greenwood & Edwards, 2006a) or binocular disparity (Greenwood & Edwards, 2006b). The role of global-motion processing is further seen in the reduced responses of MT/V5 cells to transparent motion compared with unidirectional stimuli (Snowden, Treue, Erickson, & Andersen, 1991). This reduction may reflect the lower signal intensity in transparent-motion stimuli, where half the dots move in each signal direction and can thus act as noise for detection of the other signal (Edwards & Nishida, 1999), given the sensitivity of MT/V5 cells to global-motion signal intensity (Britten, Shadlen, Newsome, & Movshon, 1993).

Within the global-motion stage, a broad range of detectors will respond to transparent-motion stimuli. The simplest means to detect transparency from this population response would be for the two highest peaks in activity to correspond to the perceived directions, as implemented by a range of models (Durant, Donoso-Barrera, Tan, & Johnston, 2006; Jasinschi, Rosenfeld, & Sumi, 1992; Nowlan & Sejnowski, 1994; Simoncelli & Heeger, 1998). For this bimodal activity to occur, detectors selective for the component transparent-motion directions must respond at a higher rate than those selective for the mean direction. However, because the direction-tuning bandwidth of MT/V5 cells averages 90° (Albright, 1984; Felleman & Kaas, 1984), transparent-motion signals with angular separations below this may produce unimodal activity through both signals activating detectors selective for the mean (Treue et al., 2000). Rather than peak detection, Treue et al. propose that transparent-motion signals could be inferred by fitting multiple Gaussian-shaped curves to the unimodal population activity. The neural mechanisms that would allow such curve fitting are unclear.

There are, nonetheless, two factors that can be used to examine the mechanisms underlying transparent-motion detection and the likelihood of either bimodal or unimodal activity being present for threshold-level angular separations. The first is the smallest angular separation that allows transparent-motion detection ($\Delta\theta_{min}$). The second is the direction-tuning bandwidth of global-motion detectors, which determines the spread of activity across the global-motion population.

1.2. Angular separation thresholds for transparency

There is considerable variation amongst prior estimates of the smallest angular separation for transparency. The lowest $\Delta\theta_{min}$ estimates come from studies using random-dot stimuli to examine direction repulsion, where values of 5–10° have been reported (Hiris & Blake, 1996; Marshak & Sekuler, 1979). However, because these experiments only required judgements for one of the directions, observers could have detected the target signal in isolation, particularly with the 1 s presentation times. These long durations may also allow the detection of relative motion between individual dots, as seen with global-flow stimuli (Williams & Sekuler, 1984) where dissimilar local-motion directions are evident despite the global motion towards the vector average.

Larger $\Delta\theta_{min}$ estimates are obtained when both signals must be detected simultaneously. For instance, angular separations around 25° were required for observers to orient two lines according to the directions in transparent-motion stimuli (Braddick et al., 2002). A larger estimate of 45° was obtained with a task requiring discrimination between one of the directions in transparent-motion stimuli and subsequent test directions (Smith, Curran, & Braddick, 1999). Finally, when observers indicated the presence of single directions after the presentation of transparent motion, experienced observers failed with angular separations below 60°, while untrained observers required separations up to 120° (Felisberti & Zanker, 2005). By ensuring the simultaneous detection of both signals, rather than one of the signals in isolation, these $\Delta\theta_{min}$ estimates are more likely to reflect the smallest detectable angular separations required for transparency.

1.3. Variation in global-motion direction-tuning bandwidths

If transparent-motion detection is dependent on the direction-tuning bandwidth of global-motion detectors, any variation in bandwidth should affect $\Delta\theta_{min}$ values. Direction-tuning anisotropy has been suggested previously as an explanation of the oblique effect for motion, whereby unidirectional discrimination thresholds are lower for cardinal than oblique directions (Ball & Sekuler, 1980; Gros, Blake, & Hiris, 1998). Because unidirectional detection thresholds are equal across all axes, this oblique effect cannot arise from variation in the number of detectors tuned to different directions. Rather, narrow direction tuning around the cardinal axes would give greater discrimination performance than broader tuning around oblique axes, without affecting detection thresholds (Gros et al., 1998). The effect of direction uncertainty around cardinal and oblique axes also suggests broader direction tuning for oblique directions (Ball & Sekuler, 1980).

Despite this psychophysical evidence, analyses of MT/V5 cells are yet to find anisotropies in either bandwidth or the distribution of preferred directions (Albright, 1984; Churchland, Gardner, Chou, Priebe, & Lisberger, 2003; Maunsell & Van Essen, 1983). In contrast, there is a strong neural basis for the oblique effect for orientation, which occurs for both detection and discrimination (Appelle, 1972). Consequently, there is evidence for both an increased number of V1 cells tuned to cardinal orientations (Furmanski & Engel, 2000; Maffei & Campbell, 1970;

Mansfield, 1974) and tighter bandwidths around cardinal axes in V1 simple cells (Li, Peterson, & Freeman, 2003). This latter finding comes from a survey of 4000 V1 cells, suggesting that similarly large samples may be required to detect anisotropy within MT/V5. Considering the evidence for anisotropies within V1, it would be surprising were this not inherited throughout the motion-processing system.

Given the logical connection between $\Delta\theta_{min}$ and global-motion direction tuning, the psychophysical evidence for bandwidth variation suggests that $\Delta\theta_{min}$ should also vary around different axes of motion. We sought to examine this relationship to elucidate the mechanisms underlying transparent-motion detection.

2. Experiment 1: Angular separation thresholds for transparent motion

Angular separation thresholds for transparency were assessed around four axes of motion. Because of the discrepancy between prior $\Delta\theta_{min}$ estimates, we devised a task that required simultaneous detection of both signals without the potential to use relative motion cues arising from differences in selected dot trajectories. The latter was ensured by pairing transparent-motion stimuli of a given angular separation and global-flow stimuli (Williams & Sekuler, 1984) consisting of a direction distribution covering the same range. A similar procedure has been used to examine speed-difference thresholds for speed-based transparency (Masson, Mestre, & Stone, 1999). Brief presentation times were used to ensure simultaneous rather than sequential detection of signals (Braddick et al., 2002; Edwards & Greenwood, 2005).

2.1. Method

2.1.1. Observers

Three observers took part in this experiment: one of the authors (JG) and two naïve observers (DW and FB). All had normal or corrected-to-normal vision with no history of visual disorders.

2.1.2. Apparatus

Stimuli were generated using a Cambridge Research Systems VSG 2/5 in a host PC, and displayed on a Sony Trinitron 20 in. monitor with a resolution of 1312×983 pixels and a refresh rate of 80 Hz. From a viewing distance of 1.5 m, the physical extent of the monitor subtended $11.3 \times 8.7°$. Stimuli were viewed binocularly in a dark room, with head movements restricted by a chin rest. Observers initiated each staircase and responded to trials via the mouse buttons. The same apparatus was used for both experiments.

2.1.3. Stimuli

Random-dot stimuli were presented within a 6.1° diameter aperture, the boundaries of which were invisible. Each aperture contained 160 dots of 0.06° diameter. This gave a dot density of 5.5 dots/deg^2, which has a low probability of local balancing (Qian et al., 1994). The background was set to mean luminance (47 cd/m^2), with dots defined by a luminance increment of 30% Weber contrast. A $0.15 \times 0.15°$ black fixation cross was provided to minimise eye movements.

To avoid the interference that can result from rapid changes in direction (Watamaniuk, Flinn, & Stohr, 2003), dots moved in a continuous direction for the entire stimulus duration. A step size of 0.23° was taken between frames. In conjunction with the low dot density, this gave a low probability of false correspondence matches (Williams & Sekuler, 1984) and is below d_{max} thresholds for transparent motion (Snowden, 1989). Each frame was presented three times to last 37.5 ms, producing a speed of 6.1°/s. This combination of frame rate and step size minimised error in the angular displacement of dots, with no difference between the accuracy of cardinal and oblique displacements. Dots that moved outside the aperture were wrapped and re-plotted in the opposite half of the aperture.

2.1.4. Procedure

A temporal two-alternative forced-choice (2AFC) procedure was used, with each interval presented for 225 ms (six frames of motion). One interval contained two transparent-motion signals with a given angular separation. The other contained a global-flow stimulus, where the direction of each dot was selected from a rectangular distribution equal to the angular separation between the comparison transparent-motion signals (see Fig. 1). For instance, with a 40° separation in the transparent-motion interval, global-flow dots could move in any of the 41 directions across this range. These latter stimuli were perceived as a noisy motion signal moving towards the vector

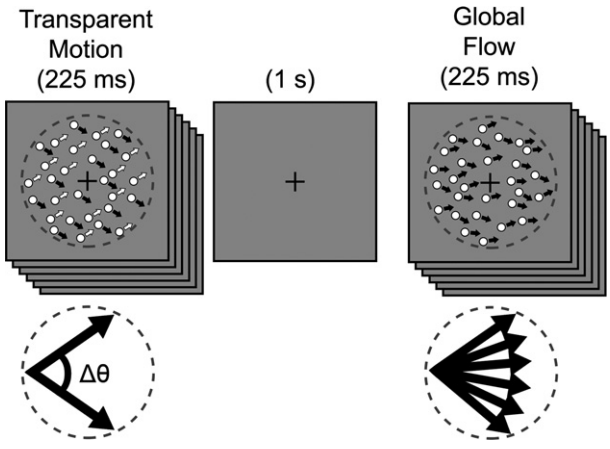

Fig. 1. Depiction of an example trial to assess angular separation thresholds for transparency. One of the two stimulus intervals randomly contained transparent motion with a given angular separation ($\Delta\theta$). With maximum signal intensity, half the dots moved in each of the two directions. The other interval contained a range of directions with the same boundaries, as shown in the lower apertures. Both had the same mean direction.

average of the distribution. With subthreshold angular separations, transparent-motion stimuli had a similar appearance. This comparison thus minimised the potential to use relative local-motion cues to perform the task. Stimulus intervals were separated by a 1 s blank interval.

Observers were required to indicate which of the two intervals, presented in random order, contained transparent motion. Angular separation began at a randomised value between 160–180° and was varied with a modified 3-down 1-up staircase procedure converging on 79% correct performance (Levitt, 1971). Eight reversal points were collected, with thresholds taken as the mean of the last six. The step size for angular changes began at 32° and was reduced after each reversal to reach 2° for the final reversals.

For each staircase, transparent-motion signals were centred on a common axis of motion, with angular separation varied around this axis to reach threshold. In pilot testing, thresholds centred on opposite directions of the same axis were identical (e.g. 0° leftwards vs. 180° rightwards). To minimise adaptation, the mean direction was thus randomly set to either extreme of the axis for each trial. Both intervals within a trial had the same mean. Four axes were examined, with the mean direction set at either end of the horizontal axis (0/180°), the vertical axis (90° upwards/270° downwards), or two oblique axes (45/225° or 135/315°). Thresholds were also assessed with the mean randomised around 360° for each trial.

Because most conditions assessed $\Delta\theta_{min}$ around a fixed axis, any variation in performance could be attributed either to this mean direction or the component directions at threshold. Thus, thresholds were also assessed with reduced signal intensity to elevate $\Delta\theta_{min}$ and separate the effect of the mean from that of the component directions. With maximum signal intensity, transparent-motion stimuli involved half the dots moving in each of the two directions, while global-flow stimuli had all dots moving within the relevant directional bandwidth. The lowered signal intensity varied slightly between observers. For JG and DW, each transparent-motion signal had an intensity of 20%, with the remaining 60% of dots moving in random directions selected from a rectangular 360° distribution. To ensure these noise dots were not a cue to the transparency interval, the equivalent number of noise dots were added to global-flow stimuli. Thus, 40% of the dots in these intervals moved within the global-flow bandwidth, while the rest moved in random directions around 360°. For FB, signal intensities were set to 25% to allow stable performance.

Initially, 10 practice staircases were completed to allow performance to stabilise. Ten estimates of threshold were collected for each condition, in random order, with no feedback given during trials.

2.2. Results and discussion

Scores in both experiments were screened for outliers, with additional staircases run when scores exceeded 2.5 standard deviations from the mean. The resulting means and standard error for the maximum signal intensity condition are displayed as a function of the mean axis of motion in Fig. 2a. A clear oblique effect is evident for all observers, with $\Delta\theta_{min}$ thresholds lower around the cardinal axes (Horz. and Vert.) than the oblique axes (R-Oblq. and L-Oblq.). This is particularly so for thresholds around the horizontal axis, which tended to be lower than vertical thresholds. Oblique thresholds did not differ from one another. For instance, FB required an angular separation of 22° around the horizontal axis, compared with 31° and 30° around oblique axes. With a randomised mean, $\Delta\theta_{min}$ ranged from 28–36°. These values do not differ from the average of the non-randomised conditions, with a 3% improvement on the non-randomised average for JG, while DW and FB show decrements of 5% and 3%, respectively.

In Fig. 2b, the means and standard error are shown for the lowered signal intensity condition. An oblique effect is again apparent, with thresholds lowest around the cardinal axes. For JG and DW, horizontal thresholds were lower than vertical, though this relationship was reversed for FB.

2.2.1. Relation to previous studies

With maximum signal intensity, $\Delta\theta_{min}$ values varied between 22–39°. As expected, these values are well above those of direction repulsion studies (Hiris & Blake, 1996; Marshak & Sekuler, 1979), due to the removal of relative local-motion cues and the brief presentations that ensure simultaneous detection of the signals. Compared with other studies that require simultaneous detection of both signals, our $\Delta\theta_{min}$ values are consistent with the 25° of Braddick et al. (2002), slightly lower than the 45° minimum specified by Smith et al. (1999) and considerably below the 60–120° of Felisberti and Zanker (2005).

The particularly high $\Delta\theta_{min}$ values in the latter study may relate to their requirement that observers indicate the presence of specific directions cued after presentation. Shifts in perceived direction resulting from direction repulsion (Marshak & Sekuler, 1979), as well as the lowered precision of direction judgements for transparency (Braddick et al., 2002), would inflate thresholds by reducing accuracy on this task. Accordingly, experiments examining perceived direction rather than reference directions (Braddick et al., 2002; Smith et al., 1999), as well as the examination of transparency in the present study, produce substantially lower $\Delta\theta_{min}$ estimates.

2.2.2. Control experiments

Before considering the implications of the oblique effect, two control conditions were run to rule out the possibility of extraneous cues being used to perform the task. One potential cue is the difference in signal intensity between the transparent-motion and global-flow stimuli (Edwards & Badcock, 1998). Particularly with narrow directional bandwidths, the effective signal intensity of global-flow stimuli would be higher than the transparent-motion

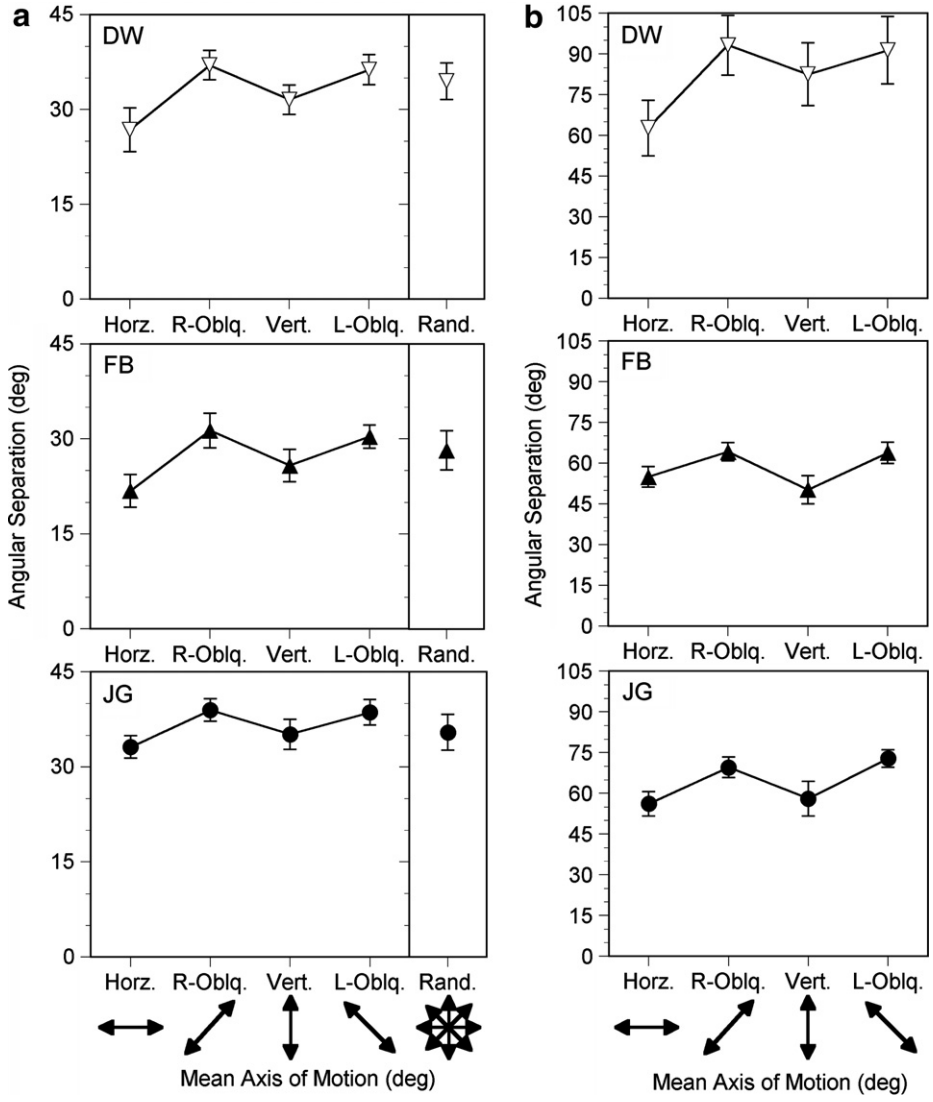

Fig. 2. Angular separation thresholds as a function of the mean axis of motion. Four axes were assessed: Horz. (0/180°), R-Oblq. (45/225°), Vert. (90/270°), and L-Oblq. (135/315°), as indicated with arrows below the *x*-axis. Data points are the average of ten staircase estimates; error bars represent one SEM. (a) Results obtained with maximum signal intensities including data obtained with a randomised mean. (b) Results with lowered signal intensities. Each transparent-motion signal had an intensity of 20% for DW and JG, and 25% for FB.

signals through stronger activation of detectors selective for the mean direction. Thus, a control condition was run with the global-flow signal intensity reduced to match one of the transparent-motion signals. To have noise in both intervals, transparent-motion stimuli were presented at 35% signal intensity, while global-flow stimuli had 35% of the dots moving within the appropriate bandwidth and the remainder as noise. The standard task (as in Fig. 1) was also run with 35% signal intensity for direct comparison, with both conditions centred on the horizontal axis. Performance did not differ substantially between the two conditions, as displayed in Fig. 3 for two observers, making it unlikely that signal intensity differences were used to perform the task.

The second control condition addressed the possibility that observers could attend to one of the transparent-motion signals in isolation. To do so, a direction skew was introduced to global-flow stimuli such that half the flow dots moved at one extreme of the directional range, equivalent to one of the transparent-motion signals. Transparent-motion signal intensities were again 35%, centred on the horizontal axis. For flow stimuli, 35% of the dots moved at one extreme of the bandwidth, with the other 35% moving within the directional bandwidth and the remainder moving as noise. The skew direction was randomised across trials, removing the potential to attend to a single direction. As displayed in Fig. 3, results did not differ from the standard condition, demonstrating that individual signals were not being used to perform the task. This is consistent with the identical performance in randomised and non-randomised mean direction conditions in the main experiment (Fig. 2a). Because the exact component directions could not be predicted in the randomised condition, attending to individual directions should have impaired performance. Together, these results demonstrate

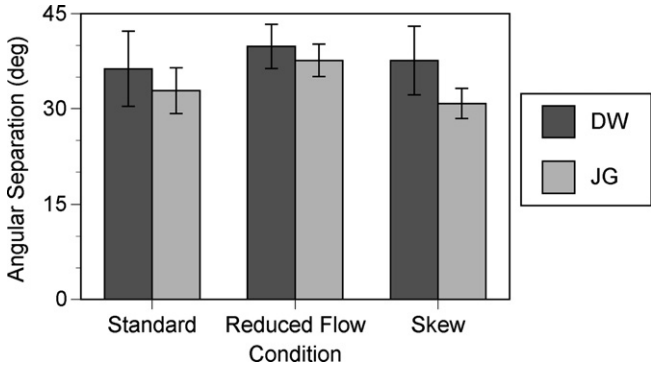

Fig. 3. Mean angular separation thresholds for the control conditions. Signal intensity in the transparent-motion interval was 35% for all conditions. The *standard* condition was identical to the main experiment. With *reduced flow*, the global-flow intensity was reduced to 35% of dots moving within this boundary, equal to one of the transparent-motion signals. For the *skew* condition, global-flow stimuli had a direction skew where half the flow dots (35% of total) moved at one extreme of the distribution.

that performance in our task was based on the detection of transparent motion.

2.2.3. Detectors underlying the oblique effect

To examine whether a subset of detectors produce the transparent-motion oblique effect, the influence of the component directions was compared with that of the mean. Because our staircases were each centred on a common axis of motion, it could be that any set of component directions around a cardinal mean produce better performance than transparent-motion detection around oblique axes. On the other hand, component directions closest to the nearest cardinal axis could give better performance than oblique component directions.

For each of the mean-axis conditions, the component directions at threshold were calculated. Examples are shown in Fig. 4a, where the component directions for JG in one cardinal (0/180°) and one oblique condition (135/315°) are displayed for both signal intensities. With maximum signal intensity, component directions were close to the mean direction for both oblique and cardinal conditions. However, the elevation of thresholds with lowered signal intensities means that component directions centred on 0/180° were further from the nearest cardinal axis than the component directions in the 135/315° oblique condition.

To quantify this pattern, the difference between component directions and the nearest cardinal axis was taken for each threshold estimate (e.g. 0° for the 0/180° mean direction condition in Fig. 4a). These scores are presented in Figs. 4b–d. With maximum signal intensity, component directions around a cardinal mean were always closer to cardinal axes than component directions with an oblique mean. In contrast, lowered signal intensities produced component directions around cardinal axes that were further from the nearest cardinal axis than components with an oblique mean. Despite this reversal, $\Delta\theta_{min}$ thresholds in both signal intensity conditions were lower when centred on cardinal mean directions than oblique means. Thus, the transparency oblique effect depends more on the mean direction than the components, suggesting that it derives from the characteristics of detectors with preferred directions centred on cardinal and oblique axes.

2.2.4. Basis of the oblique effect for transparency

As discussed earlier, the unidirectional oblique effect has been attributed to variation in the direction-tuning bandwidth of cells tuned to cardinal and oblique axes, rather than variation in the number of cells with preferred directions at these axes. For transparent-motion detection, broader bandwidths around oblique axes would increase the sensitivity of these detectors to the two components, and thus the likelihood of unimodal activity that is indistinguishable from unidirectional motion. However, variation in the number of cells tuned to cardinal and oblique directions could also affect transparency by giving greater resolution of the separation between transparent-motion signals around cardinal axes compared with oblique axes.

To compare the effect of these two factors, a simple model was constructed with an array of direction-selective filters simulating global-motion detectors. The direction-tuning bandwidths of these filters were produced with von Mises functions, the circular analogue of a Gaussian curve:

$$y = \exp(b\cos(\theta - \theta_p)) \quad (1)$$

Here, b determines the tuning bandwidth, θ represents direction, and θ_p is the peak location of the curve. Each curve was normalised to have a base at 0 and a peak at 1 by subtracting the minimum value and dividing by the maximum. This gave an array of detectors, as plotted in Fig. 5a, which could vary in number (and subsequent spacing between preferred directions) as well as bandwidth. Peak directions of detectors were initially evenly distributed across direction space.

Responses to transparent-motion stimuli were simulated by multiplying the direction of each dot by the sensitivity of detectors. There was no noise in the model, with the response to each dot summed linearly (Treue et al., 2000) to give responses between 0-1 for each detector. Fig. 5b displays the responses to transparent motion with different angular separations, plotted according to the preferred directions of detectors. While large angular separations produce two prominent activity peaks, decreasing the angular separation reduces the prominence of peaks until the activity from each component direction overlaps sufficiently to produce a unimodal distribution.

For a given detector population, the angular separation at which activity shifted from bimodal to unimodal (the unimodal angle) was taken as an index of transparent-motion detection. This was quantified as the angle at which peak activity became equal to the activity of detectors at the mean direction. Results from a range of simulations

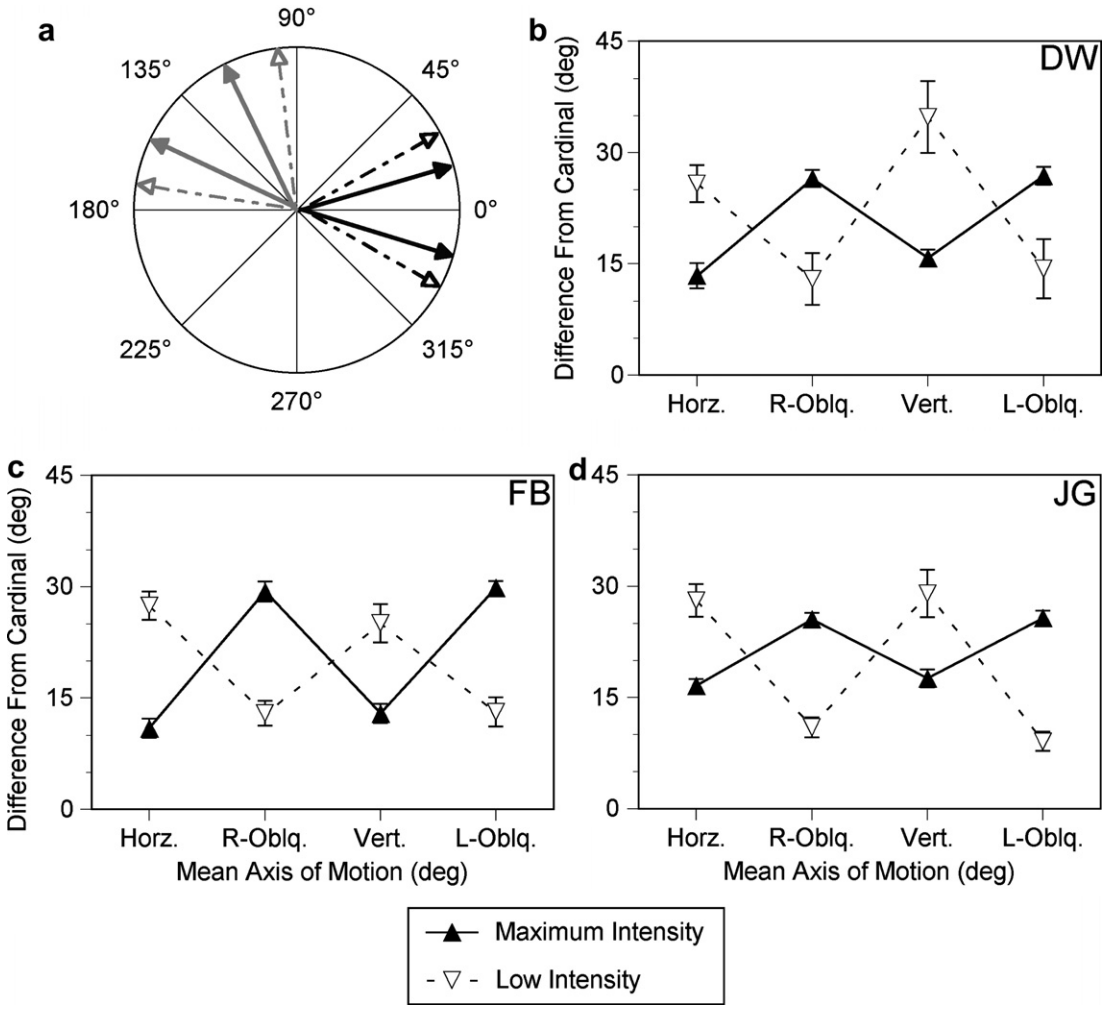

Fig. 4. Plots of the directions present at threshold and their divergence from the nearest cardinal axis. (a) Example thresholds for JG in two conditions, shown by the angular position of arrows. Black arrows show threshold directions around a 0° mean (0/180° mean-axis condition); grey arrows around a 135° mean (135/315° mean axis). Solid lines depict conditions with maximum signal intensity; lowered intensity conditions have broken lines. (b) The difference between component directions and the nearest cardinal axis for DW, (c) FB, and (d) JG. Each data point is the average of ten estimates of threshold.

are displayed in Fig. 5c, where each point represents the unimodal angle produced by a set number of detectors with identical bandwidths. Each line shows the effect of varying bandwidth on a fixed number of detectors distributed evenly across direction space, with the difference between preferred directions indicated in the figure legend. Increasing the number of detectors shifted curves downwards, as smaller angular separations produced bimodal population activity. This improvement reached a maximum with 14–15 broadly tuned detectors (where peak directions differ by 24–25°), and around 20–30 narrowly tuned detectors (differing by 12–18°). For variation in the number of detectors to affect angular separation thresholds, the preferred directions of MT/V5 cells would thus have to differ by more than 12°. The distribution of preferred directions in MT/V5 is much more continuous than these large steps, with variation both within and across the direction-selective columns (Albright, Desimone, & Gross, 1984). In contrast, bandwidth had a strong effect on the unimodal angle regardless of the number of detectors, with narrow bandwidths producing bimodality with smaller angular separations than populations with broad bandwidths.

This is further illustrated by the precise values of detector spacing and bandwidth that produce our $\Delta\theta_{min}$ values. With bandwidth fixed at 25° FWHM, the difference between peak directions must vary from 7–15° around cardinal axes to 14–19° around oblique axes to account for our data. As before, these values are far too coarse to be physiologically realistic. In comparison, for any number of detectors greater than 30, the observed $\Delta\theta_{min}$ variation could be produced by bandwidths of 25–39° around cardinal axes and 37–46° around oblique axes. These values are within the range of observed MT/V5 bandwidths, where FWHM values from 20° up to more than 120° have been reported (Albright, 1984; Felleman & Kaas, 1984).

Though the above simulations compare distinct populations with constant detector spacing and bandwidth, similar results occur when varying these factors within the same

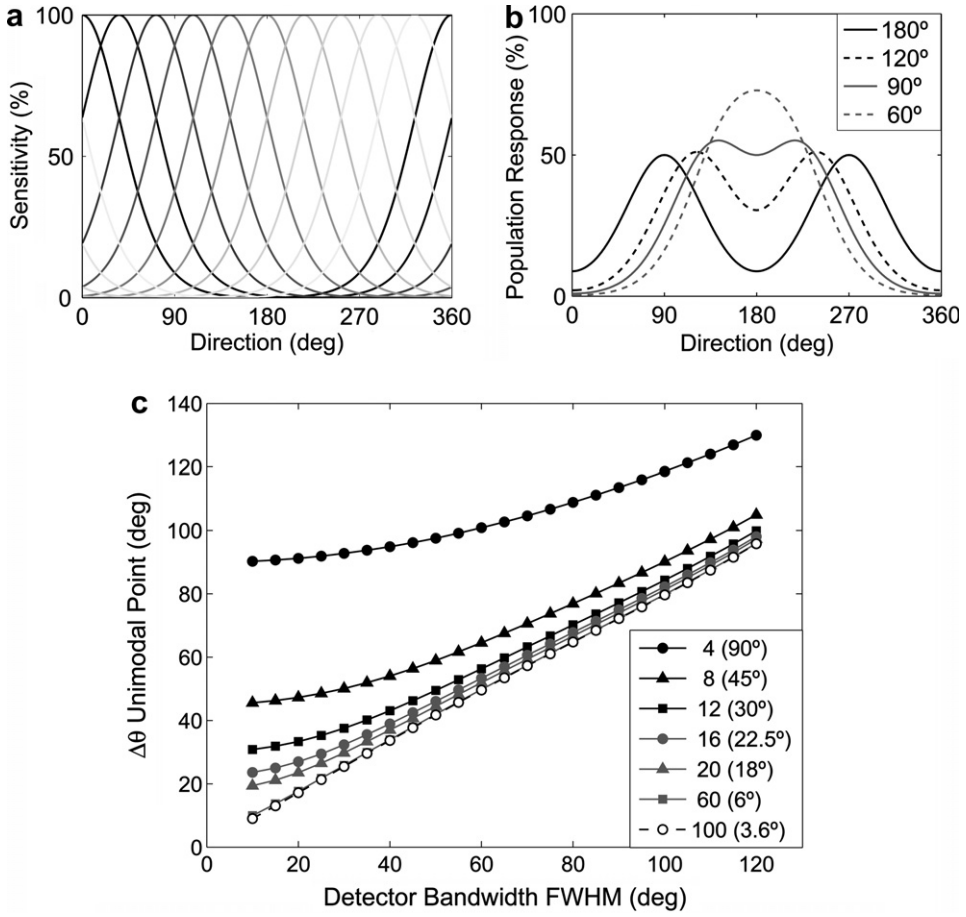

Fig. 5. Simulations of global-motion processing with transparent-motion stimuli. (a) An example array of 10 detectors with bandwidths of 90° FWHM. (b) Example population activity from 100 detectors with 90° FWHM where peak directions were equally distributed, differing by 3.6°. Responses to four angular separations are shown, with bimodal activity evident for the three largest separations. (c) The angular separation at which activity shifts from bimodal to unimodal (the unimodal angle) as a function of both bandwidth and number of detectors (with constant peak direction differences). The *x*-axis plots different bandwidth values, with each line representing populations differing in the number of detectors (indicated in the figure legend; numbers in brackets give the difference between preferred directions). With 100 detectors or more, population activity became unimodal at an angular separation equal to 80–85% of the FWHM of detectors.

population. Distributions of peak direction spacing and bandwidth were modified by a sine wave function[1] centred on a value of 1, with the minima aligned with cardinal directions to produce the smallest peak separations or bandwidth values for cardinal detectors. Regardless of the sine wave amplitude, variation in detector spacing had no effect with more than 25 detectors, with an average peak direction spacing of 15°. Bandwidth variation had a strong effect regardless of the number of detectors or the absolute values of bandwidth.

Together, these simulations demonstrate that the most plausible way to account for $\Delta\theta_{min}$ variation is through anisotropy in the bandwidth of global-motion detectors. This was directly tested in Experiment 2.

[1] Functions other than sine waves produce quantitative differences in the unimodal angle, though the qualitative result is the same.

3. Experiment 2: Direction tuning around cardinal and oblique axes

The direction tuning of global-motion detectors was examined using adaptation and subsequent elevation of detection thresholds. Consistent with the broad direction tuning of global-motion detectors, adaptation to unidirectional motion elevates detection thresholds for a range of test directions, with elevation decreasing as the test direction diverges from the adaptor (Raymond, 1993). If there is a difference between the bandwidth of cardinal and oblique detectors, adaptation to an oblique direction should elevate thresholds for a wider range of test directions than cardinal adaptation.

3.1. Method

3.1.1. Observers

Observers FB and JG participated in this experiment.

3.1.2. Stimuli

The stimulus configuration was modified slightly from Experiment 1 to maximise adaptation. Because high dot density gives a more accurate measure of adaptation (Castet, Keeble, & Verstraten, 2002), the aperture diameter was decreased to 3.8° and the number of dots increased to 200, producing a dot density of 17.5 dots/deg^2. Weber contrast was also increased to 100% to facilitate adaptation (Keck, Palella, & Pantle, 1976). Other parameters were identical to those of Experiment 1.

3.1.3. Procedure

Each trial consisted of three intervals. The first was the adaptation interval, with dots moving in a single direction either towards the right (cardinal, 0°) or the upper right (oblique, 45°). Adaptation lasted 100 s to begin each staircase, with 5 s top-up intervals preceding subsequent trials. Dots were static in this interval for non-adaptation trials. The two test intervals were each presented for 150 ms (four frames) with a 500 ms inter-stimulus interval.

Of the two test intervals, one randomly contained a unidirectional global-motion signal amongst noise, with noise directions selected from a 360° rectangular distribution. The other consisted solely of noise dots. Observers made a 2AFC decision regarding which interval contained the signal. The proportion of signal dots was varied using a 3-down 1-up staircase. Initially, 120 signal dots were present (60% intensity), with steps of 12 dots for initial signal intensity changes that decreased to a single dot for the final reversals.

Each staircase assessed the global-motion detection threshold for one test direction. For JG, six test directions were examined for each adaptation condition. With 0° adaptation, test directions were 0°, 10°, 20°, 30°, 40° and 60°, with test directions of 45°, 55°, 65°, 75°, 85° and 105° examined following 45° adaptation. FB completed three test directions for each adaptation condition—0°, 20° and 60° with 0° adaptation, and 45°, 65° and 85° following 45° adaptation. Ten staircases were completed for each test direction, both with and without adaptation.

3.2. Results and discussion

Without adaptation, thresholds for both observers were reached with 30–40 signal dots out of 200. Thresholds were similar across all test directions, consistent with previous reports of isotropy for motion detection (Ball & Sekuler, 1980; Gros et al., 1998). Threshold elevation ratios were obtained by dividing post-adaptation thresholds by the mean non-adaptation threshold for each test direction, as displayed in Fig. 6. Thresholds were maximally elevated for test stimuli moving in the same direction, with decreasing elevation as the test direction was angled away from the adaptor. When test and adapting directions were matched, threshold elevation was slightly stronger following oblique adaptation. This difference increased as the test direction diverged from the adaptor, due to the more rapid decrease in threshold elevation for cardinal adaptation. Overall, adaptation to oblique motion produced threshold elevation for a wider range of test directions than cardinal adaptation.

For each data set, logistic functions were fit to determine the half-width at half-maximum, with standard error terms produced using a bootstrap procedure (Efron & Tibshirani, 1993). For JG, half-widths were 12° for cardinal adaptation and 21° for oblique, while FB produced half-widths of 18° for cardinal and 34° for oblique adaptation. This confirms that oblique adaptation produced threshold elevation in a wider range of test directions than cardinal adaptation. The difference between observers could reflect either individual bandwidth differences, or the sparse sampling of test directions with FB. Nonetheless, oblique bandwidth estimates were approximately twice the size of cardinal estimates for both observers.

Doubling these estimates gives full-width at half-maximum values of 24–36° for cardinal detectors and 42–68° for oblique detectors. These FWHM values are close to the predictions of our model, which were between 25–39° for cardinal detectors and 37–46° for oblique detectors. However, both these predictions and our obtained bandwidth values are substantially narrower than those obtained by Raymond (1993). This is of particular interest given the close relation between our narrow estimates of bandwidth and angular separation thresholds, as we will consider further in Section 4.3.

4. General discussion

The experiments reported herein demonstrate an oblique effect for transparent-motion detection, with lower angular separation thresholds around cardinal axes than around oblique axes (Experiment 1). Subsequent modelling suggested this is most likely due to broader direction tuning around the oblique axes. Results from Experiment 2 were consistent with this prediction, with adaptation to an oblique direction producing threshold elevation in a wider range of test directions than cardinal adaptation.

These results give three main insights into transparent-motion detection. First, transparent-motion detection is strongly linked with the bandwidth of global-motion detectors. Second, the characteristics of detectors selective for the mean direction of transparent-motion stimuli are more important than those selective for other directions, including the component directions themselves. Finally, our narrow estimates of bandwidth suggest that transparent-motion detection could rely on a bimodal activity distribution within the global-motion stage. These issues will be considered in turn.

4.1. Direction tuning and the oblique effect

Together, these experiments demonstrate the dependence of transparent-motion detection on the direction tuning of global-motion detectors. Broader bandwidths

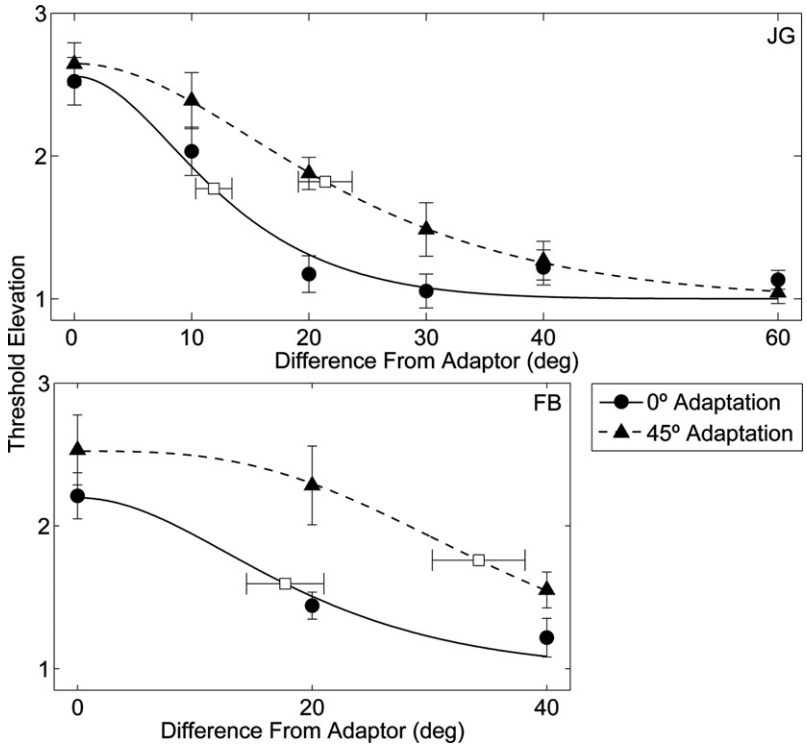

Fig. 6. The effect of adaptation on thresholds for global-motion detection, as a function of the difference between test and adapting directions. Threshold elevation ratios were obtained by dividing each post-adaptation threshold by the mean non-adaptation threshold for the same test direction. Data points are the average of ten staircases; error bars are one SEM. Logistic curves were fit to determine the half-width at half-maximum (open squares), with standard error terms determined with a bootstrap procedure. For both observers, adaptation to 45° motion (triangles) produced threshold elevation in a wider range of test directions than 0° adaptation (circles).

around oblique axes would make small angular separations more difficult to detect by increasing the spread of activity across the global-motion population, as seen in our model. This is consistent with the purported role of direction tuning in the oblique effect for unidirectional discrimination (Ball & Sekuler, 1980; Gros et al., 1998) as well as the differential effect of direction uncertainty around cardinal and oblique axes (Ball & Sekuler, 1980).

This bandwidth variation should occur for global-motion detectors, given both the dependence of transparent-motion detection on this stage and the effect of adaptation on global-motion detection thresholds in Experiment 2. It is possible that bandwidth anisotropy may initially arise within the local-motion stage (e.g. Dakin, Mareschal, & Bex, 2005), particularly given the evidence for an oblique effect for orientation (e.g. Appelle, 1972). However, our results indicate that this must be carried through to global-motion detectors.

Given this psychophysical evidence, the lack of evidence for bandwidth variation in MT/V5 may relate to the small sample sizes used in previous studies (Albright, 1984; Churchland et al., 2003; Maunsell & Van Essen, 1983), compared to the sample size required to detect bandwidth anisotropy in V1 (Li et al., 2003). Large samples would be particularly important were this anisotropy only present for a subset of MT/V5 detectors, as in V1 simple cells (Li et al., 2003). It is also possible that bandwidth anisotropy arises from interactions between detectors, such as inhibition between detectors tuned to different directions (e.g. Ringach, Hawken, & Shapley, 1997). Greater inhibition around cardinal axes could narrow the bandwidth of these detectors compared with oblique detectors. However, the opposite pattern occurs for direction repulsion, which has also been attributed to direction-specific inhibition, with greater repulsion for oblique directions than cardinal (Hiris & Blake, 1996). A more detailed analysis of MT/V5 cells and their interactions may be required to find a physiological correlate of the observed bandwidth anisotropy.

4.2. The role of the mean direction in transparent-motion detection

Analysis of our angular separation thresholds revealed that performance relied more on the mean direction than the component directions within stimuli. This is attributable to the bandwidth differences found for detectors with these preferred directions, particularly if transparent-motion detection requires multiple activity peaks, as considered in Section 4.3. For a given angular separation, detectors selective for the mean direction with broad bandwidths would be more strongly activated than detectors with narrow direction tuning. Increased responses from these central detectors would make the peaks of population activity harder to discern, particularly as the angular

separation decreased. Variation in the bandwidth of detectors with preferred directions away from the mean would have less effect due to the decreased likelihood of activation from both signals.

This dependence on the mean direction is consistent with experiments using transparent-motion stimuli composed of two global-flow distributions. Though detection was impaired as the bandwidth of the flow distributions increased, performance depended more on the separation between the boundaries of the flow distributions than the separation between each of the component means (Smith et al., 1999). That is, separation between the two distributions was more important than the effective strength of the components. As in the present study, this is likely to reflect the importance of detectors selective for the mean in determining whether the population activity is unimodal or bimodal.

More generally, reliance on a subset of detectors within the global-motion population is also seen in other tasks. For instance, while unidirectional detection is impaired most by adaptation to directions matching the stimulus, discrimination is most affected by adaptation to directions 40–60° from the target direction (Hol & Treue, 2001). Analyses of the most informative MT/V5 cells for detection and discrimination yield similar results (Newsome, Britten, & Movshon, 1989; Purushothaman & Bradley, 2005). The visual system, logically enough, appears to rely on the most informative cells within a population for a given task.

4.3. Models of transparent-motion detection

Results from the current study present difficulties for the model of transparent-motion detection proposed by Treue et al. (2000). Because the averaged MT/V5 population activity was unimodal with angular separations below 90°, transparent-motion detection was argued to arise through curve-fitting procedures that infer multiple Gaussian profiles based on the average bandwidth of detectors. One problem posed by our results is that these curve-fitting processes would have to account for the observed bandwidth anisotropy. Were the visual system able to do so, transparent-motion detection would not vary for different axes of motion, as curve fitting should be equally efficient with broader assumed bandwidths. The transparency oblique effect suggests either that these processes erroneously assume a constant underlying bandwidth, or that other processes are being used.

Our bandwidth estimates are also considerably more narrow than the average bandwidth of MT/V5 cells (Albright, 1984; Felleman & Kaas, 1984), as well as some psychophysical estimates (e.g. Raymond, 1993), which raises the possibility that bimodal activity is present at angular separations below 90°. In particular, the correspondence between our bandwidth estimates and $\Delta\theta_{min}$ values suggests that bimodal activity could be utilised for transparent-motion detection, as proposed by a range of models (Durant et al., 2006; Jasinschi et al., 1992; Nowlan & Sejnowski, 1994; Simoncelli & Heeger, 1998). Around the horizontal axis, detectors were estimated to have bandwidths of 24–36° FWHM, while observers failed to detect angular separations below 20–30°. Detectors selective for oblique directions were estimated to have bandwidths of 42–68°, while $\Delta\theta_{min}$ values were 30–40°. When these bandwidths are used in our global-motion model (Fig. 5), population activity shifts from bimodal to unimodal at angular separations close to the observed threshold levels.

Though adaptation may reduce the direction-tuning bandwidth of MT/V5 cells (Kohn & Movshon, 2004), several factors make this unlikely to account for our narrow bandwidth estimates. First, adaptation to gratings moving in the preferred direction of these cells halved their bandwidths. If we assume an average of 90°, cardinal bandwidths would have to be reduced by more than two-thirds to produce our estimates. Second, Kohn and Movshon note that adaptation with random-dot stimuli did not produce bandwidth reduction (Kohn & Movshon, 2004, p. 769). Finally, broad estimates of bandwidth have been reported by other psychophysical studies using adaptation, including 50–60° (Hol & Treue, 2001), 60–70° (Maurer, Heinrich, & Bach, 2004), and 70–80° (Raymond, 1993).

The variability between psychophysical bandwidth estimates demonstrates a strong dependence on both stimulus parameters and task demands. In particular, the marked difference between our data and that of Raymond (1993) is likely to reflect the differences in stimulus parameters. Raymond (1993) presented motion frames for 100 ms each, with a dot speed of 0.9°/s. Presenting our stimuli with these parameters, using the same procedure as above, produced a broader cardinal FWHM value of 53° for JG. However, these parameters also produced the percept of discontinuous motion, which indicates the presence of additional spatiotemporal frequency components (Watson, Ahumada, & Farrell, 1986), and has been shown to increase adaptation (Castet et al., 2002). The bandwidth estimates of Raymond (1993) may thus have been inflated, at least in part, through adaptation of a greater range of detectors with differing spatiotemporal tuning. Task demands are also likely to influence the range of active detectors, given the differential weighting of detectors for different psychophysical tasks (Hol & Treue, 2001). Thus, rather than being a direct index of the bandwidth of individual motion detectors, psychophysical estimates reflect the spread of population activity produced by detectors selective for the stimuli in question, as assessed with a particular task.

The correspondence between our $\Delta\theta_{min}$ thresholds and bandwidth estimates is likely to relate to the close matching of parameters between the two experiments. Such stimulus dependence may also explain the lack of bimodality in the averaged data of Treue et al. (2000), given that their estimates of population activity were obtained with parameters matched to the preferences of individual cells. Receptive-field position may also be important, as transparent-motion signals tend to be averaged outside the fovea (De Bruyn, 1997). Were the entire population tested

with the same stimulus, the population response may reflect more closely the output of detectors subserving the perception of transparent motion. In particular, the response of detectors with narrow bandwidths could produce bimodal activity at angular separations close to the $\Delta\theta_{\min}$ thresholds obtained in the present study.

Acknowledgments

This work was supported by the Australian Research Council through the ARC Centre of Excellence for Visual Science (CE0561903). An Australian Postgraduate Award also supported the first author.

References

Albright, T. D. (1984). Direction and orientation selectivity of neurons in visual area MT of the macaque. *Journal of Neurophysiology, 52*, 1106–1130.

Albright, T. D., Desimone, R., & Gross, C. G. (1984). Columnar organization of directionally selective cells in visual area MT of the macaque. *Journal of Neurophysiology, 51*, 16–31.

Appelle, S. (1972). Perception and discrimination as a function of stimulus orientation: the 'oblique effect' in man and animals. *Psychological Bulletin, 78*, 266–278.

Ball, K., & Sekuler, R. (1980). Models of stimulus uncertainty in motion perception. *Psychological Review, 87*, 435–469.

Braddick, O. J., Wishart, K. A., & Curran, W. (2002). Directional performance in motion transparency. *Vision Research, 42*, 1237–1248.

Britten, K. H., Shadlen, M. N., Newsome, W. T., & Movshon, J. A. (1993). Responses of neurons in macaque MT to stochastic motion signals. *Visual Neuroscience, 10*, 1157–1169.

Castet, E., Keeble, D. R. T., & Verstraten, F. A. J. (2002). Nulling the motion aftereffect with dynamic random-dot stimuli: limitations and implications. *Journal of Vision, 2*, 302–311.

Churchland, A. K., Gardner, J. L., Chou, I., Priebe, N. J., & Lisberger, S. G. (2003). Directional anisotropies reveal a functional segregation of visual motion processing for perception and action. *Neuron, 37*, 1001–1011.

Dakin, S. C., Mareschal, I., & Bex, P. J. (2005). An oblique effect for local motion: psychophysics and natural movie statistics. *Journal of Vision, 5*, 878–887.

De Bruyn, B. (1997). Blending transparent motion patterns in peripheral vision. *Vision Research, 37*, 645–648.

Durant, S., Donoso-Barrera, A., Tan, S., & Johnston, A. (2006). Moving from spatially segregated to transparent motion: a modelling approach. *Biology Letters, 2*, 101–105.

Edwards, M., & Badcock, D. R. (1998). Discrimination of global-motion signal strength. *Vision Research, 38*, 3051–3056.

Edwards, M., & Greenwood, J. A. (2005). The perception of motion transparency: a signal-to-noise limit. *Vision Research, 45*, 1877–1884.

Edwards, M., & Nishida, S. (1999). Global-motion detection with transparent-motion signals. *Vision Research, 39*, 2239–2249.

Efron, B., & Tibshirani, R. J. (1993). *An introduction to the bootstrap*. London: Chapman & Hall.

Felisberti, F. M., & Zanker, J. M. (2005). Attention modulates perception of transparent motion. *Vision Research, 45*, 2587–2599.

Felleman, D. J., & Kaas, J. H. (1984). Receptive-field properties of neurons in middle temporal visual area (MT) of owl monkeys. *Journal of Neurophysiology, 52*, 488–513.

Furmanski, C. S., & Engel, S. A. (2000). An oblique effect in human primary visual cortex. *Nature, 3*, 535–536.

Greenwood, J. A., & Edwards, M. (2006a). An extension of the transparent-motion detection limit using speed-tuned global-motion systems. *Vision Research, 46*, 1440–1449.

Greenwood, J. A., & Edwards, M. (2006b). Pushing the limits of transparent-motion detection with binocular disparity. *Vision Research, 46*, 2615–2624.

Gros, B. L., Blake, R., & Hiris, E. (1998). Anisotropies in visual motion perception: a fresh look. *Journal of the Optical Society of America. A, Optics, Image Science, and Vision, 15*, 2003–2011.

Hiris, E., & Blake, R. (1996). Direction repulsion in motion transparency. *Visual Neuroscience, 13*, 187–197.

Hol, K., & Treue, S. (2001). Different populations of neurons contribute to the detection and discrimination of visual motion. *Vision Research, 41*, 685–689.

Jasinschi, R., Rosenfeld, A., & Sumi, K. (1992). Perceptual motion transparency: the role of geometrical information. *Journal of the Optical Society of America. A, Optics, Image Science, and Vision, 9*, 1865–1879.

Keck, M. J., Palella, T. D., & Pantle, A. (1976). Motion aftereffect as a function of the contrast of sinusoidal gratings. *Vision Research, 16*, 187–191.

Kohn, A., & Movshon, J. A. (2004). Adaptation changes the direction tuning of macaque MT neurons. *Nature Neuroscience, 7*, 764–772.

Levitt, H. (1971). Transformed up-down methods in psychoacoustics. *Journal of the Acoustical Society of America, 49*, 467–477.

Li, B., Peterson, M. R., & Freeman, R. D. (2003). Oblique effect: a neural basis in the visual cortex. *Journal of Neurophysiology, 90*, 204–217.

Maffei, L., & Campbell, F. W. (1970). Neurophysiological localization of the vertical and horizontal visual coordinates in man. *Science, 167*, 386–387.

Mansfield, R. J. W. (1974). Neural basis of orientation perception in primate vision. *Science, 186*, 1133–1135.

Marshak, W., & Sekuler, R. (1979). Mutual repulsion between moving visual targets. *Nature, 205*, 1399–1401.

Masson, G. S., Mestre, D. R., & Stone, L. S. (1999). Speed tuning of motion segmentation and discrimination. *Vision Research, 39*, 4297–4308.

Maunsell, J. H. R., & Van Essen, D. C. (1983). Functional properties of neurons in middle temporal visual area of the macaque monkey I. Selectivity for stimulus direction, speed, and orientation. *Journal of Neurophysiology, 49*, 1127–1147.

Maurer, J. P., Heinrich, T. S., & Bach, M. (2004). Direction tuning of human motion detection determined from a population model. *European Journal of Neuroscience, 19*, 3359–3364.

Newsome, W. T., Britten, K. H., & Movshon, J. A. (1989). Neuronal correlates of a perceptual decision. *Nature, 341*, 52–54.

Nowlan, S. J., & Sejnowski, T. J. (1994). Filter selection model for motion segmentation and velocity integration. *Journal of the Optical Society of America. A, Optics, Image Science, and Vision, 11*, 3177–3200.

Purushothaman, G., & Bradley, D. C. (2005). Neural population code for fine perceptual decisions in area MT. *Nature Neuroscience, 8*, 99–106.

Qian, N., Andersen, R. A., & Adelson, E. H. (1994). Transparent motion perception as detection of unbalanced motion signals I. Psychophysics. *Journal of Neuroscience, 14*, 7357–7366.

Raymond, J. E. (1993). Movement direction analysers: independence and bandwidth. *Vision Research, 33*, 767–775.

Ringach, D. L., Hawken, M. J., & Shapley, R. (1997). Dynamics of orientation tuning in macaque visual cortex. *Nature, 387*, 281–284.

Simoncelli, E. P., & Heeger, D. J. (1998). A model of neuronal responses in visual area MT. *Vision Research, 38*, 743–761.

Smith, A. T., Curran, W., & Braddick, O. J. (1999). What motion distributions yield global transparency and spatial segmentation? *Vision Research, 39*, 1121–1132.

Snowden, R. J. (1989). Motions in orthogonal directions are mutually suppressive. *Journal of the Optical Society of America. A, Optics, Image Science, and Vision, 6*, 1096–1101.

Snowden, R. J., Treue, S., Erickson, R. G., & Andersen, R. A. (1991). The response of area MT and V1 neurons to transparent motion. *Journal of Neuroscience, 11*, 2768–2785.

Snowden, R. J., & Verstraten, F. A. J. (1999). Motion transparency: making models of motion perception transparent. *Trends in Cognitive Sciences, 3*, 369–377.

Treue, S., Hol, K., & Rauber, H. (2000). Seeing multiple directions of motion—physiology and psychophysics. *Nature Neuroscience, 3*, 270–276.

Watamaniuk, S. N. J., Flinn, J., & Stohr, R. E. (2003). Segregation from direction differences in dynamic random-dot stimuli. *Vision Research, 43*, 171–180.

Watson, A. B., Ahumada, A. J., & Farrell, J. E. (1986). Window of visibility: a psychophysical theory of fidelity in time-sampled visual motion displays. *Journal of the Optical Society of America. A, Optics, Image Science, and Vision, 3*, 300–307.

Williams, D., & Sekuler, R. (1984). Coherent global motion percepts from stochastic local motions. *Vision Research, 24*, 55–62.